

Original Article

Determination of split renal function by PSMA imaging: comparison of ^{68}Ga -PSMA-11 PET with $^{99\text{m}}\text{Tc}$ -MAG3 scintigraphy

Florian Rosar¹, Peter Pauly¹, Martin Ries¹, Andrea Schaefer-Schuler¹, Stephan Maus¹, Mathias Schreckenberger², Fadi Khreish¹, Samer Ezziddin¹

¹Department of Nuclear Medicine, Saarland University, Homburg, Germany; ²Department of Nuclear Medicine, University of Mainz, Mainz, Germany

Received April 24, 2020; Accepted September 8, 2020; Epub October 15, 2020; Published October 30, 2020

Abstract: MAG3 scintigraphy with determination of split renal function (SRF) is a standard procedure in patients with metastasized castration-resistant prostate carcinoma (mCRPC) undergoing PSMA radioligand therapy (PSMA-RLT). These patients also receive frequent PSMA PET/CT scans for staging and follow up. PSMA is not only overexpressed in prostate cancer epithelial cells, but also physiologically overexpressed in the proximal tubular cells of the kidney. This study investigates the utility of PSMA-targeted imaging for determination of relative renal function. mCRPC patients (n = 97) having received ^{68}Ga -PSMA-11 PET/CT and $^{99\text{m}}\text{Tc}$ -MAG3 scintigraphy in close temporal relationship were included in this retrospective study. PSMA-PET-derived SRF was calculated according to the bilateral renal PSMA content (total kidney PSMA = SUVmean \times volume), MAG3-based SRF (SRF_{MAG3}) using the common standard integral method of the renal secretion phase. The agreement of SRF_{PSMA} and SRF_{MAG3} was statistically tested using Pearson correlation and Bland-Altman analysis. The correlation between both SRF assessment methods was highly significant (P < 0.001) with r=0.91. Bland-Altman analysis confirmed agreement of the measurements. High correlation and agreement were also observed in the subgroup analyses of patients with normal and reduced renal function (r=0.81, P < 0.001 and r=0.98, P < 0.001). Renal tubular PSMA expression allows assessment of split renal function by ^{68}Ga -PSMA-11 PET/CT imaging. Additional MAG3 scintigraphy for the purpose of quantifying relative renal function contribution may be spared in settings where PSMA PET is performed; this insight could save time and unnecessary examinations.

Keywords: Split renal function, PSMA, MAG3, prostate cancer, PET/CT

Introduction

Prostate carcinoma is one of the most frequent malignant diseases in men [1]. Prostate specific membrane antigen (PSMA), a type II transmembrane protein [2], is commonly overexpressed on the surface of prostate carcinoma cells [3-5]. This makes PSMA an important target for diagnostic imaging and therapy [6]. PSMA imaging, particularly using ^{68}Ga -PSMA-11 as PET/CT tracer, has proven its validity in staging of prostate cancer [7, 8] and therapy monitoring in advanced disease [9, 10]. Likewise, radioligand therapy (RLT) with ^{177}Lu labelled PSMA ligands (PSMA-RLT) is becoming increasingly important, predominantly in late stage of metastasized castration-resistant prostate

cancer (mCRPC). PSMA-RLT yields impressive results in the palliative setting [11, 12]. However, renal tracer uptake due to physiologic overexpression of PSMA in the proximal tubules [13-15] leads to minor radiation doses of the kidney, and might at least theoretically induce radiation-related nephrotoxicity [16, 17]. While recent studies have not confirmed significant short-term damage to the kidneys resulting from PSMA-RLT [18], the risk for long-term complications has still to be investigated. This proves challenging in a cohort with a limited life-time expectancy and scarce follow up data.

Renal function is closely monitored in patients undergoing PSMA-RLT. The easiest method to assess renal function in clinical routine is esti-

PSMA PET based split renal function

Table 1. Patient characteristics

| Characteristics | |
|--------------------------|----------|
| Number of patients | 97 |
| Age | (years) |
| min | 46 |
| max | 89 |
| mean | 70 |
| Metastases | (n) |
| bone | 90 |
| lymph nodes | 71 |
| liver | 20 |
| lung | 15 |
| others | 15 |
| Previous therapy | (n) |
| first line chemotherapy | 62 |
| second line chemotherapy | 22 |
| ADT | 95 |
| eGFR | (ml/min) |
| min | 26.8 |
| max | 118.9 |
| mean | 78.0 |
| < 60 ml/min | n=20 |
| ≥ 60 ml/min | n=77 |
| PSA | (ng/ml) |
| min | 0.21 |
| max | 4525 |
| mean | 477 |
| median | 217 |

mating glomerular filtration rate (eGFR) using the modification of diet in renal disease (MDRD) formula [19], based on renal retention parameter creatinine. However, this method does not provide information on the relative (side-related) distribution of renal function and outflow conditions. The current standard and well-established method for assessment of split renal function (SRF) and outflow conditions is dynamic renal scintigraphy using ^{99m}Tc labelled MAG3 (mercaptoacetyltriglycine). MAG3 is almost exclusively excreted by secretion in the proximal tubules of the kidney [20], giving an accurate estimation of tubular renal function which can be used to determine split renal function. Split renal function, also known as differential renal function, describes the relative proportion of each kidney on total renal function. Issues with MAG3 scintigraphy may arise from its time-consuming nature with commonly 30-50 minutes per examination and potential

distress to mCRPC patients often suffering from painful skeletal metastases.

The described clinical setting encouraged us to investigate the utility of PSMA-targeted imaging for determination of relative renal function by comparing PSMA-PET-derived SRF and standard MAG3-based SRF. We evaluate retrospectively this approach in a patient cohort of mCRPC patients having undergone both imaging modalities.

Materials and methods

In this retrospective study we calculated split renal function using PSMA PET/CT (SRF_{PSMA}) and compared the results to MAG3 derived split renal function (SRF_{MAG3}). The study was performed in accordance with the Declaration of Helsinki and with national regulations. Approval of the retrospective analysis was waived by the local ethics committee. All patients provided written informed consent for the examinations and for scientific analysis and publication of data.

Patients

In total, n=97 patients treated with ^{177}Lu -PSMA-RLT in the advanced mCRPC setting were included in this study. Every patient obtained PSMA PET/CT and MAG3 scintigraphy in close temporal relationship within a period of 1 week. **Table 1** gives a detailed overview of the patient cohort.

Imaging methods

^{68}Ga -PSMA-11 PET/CT: Each patient of this study (n=97) received a ^{68}Ga -PSMA-11-PET/CT with a mean intravenously injected activity of 121 ± 15 MBq of a ^{68}Ga -PSMA-11. The incubation time between injection and PET acquisition was 60 minutes. No additional contrast media or diuretics were applied. PET datasets were acquired on a Biograph 40 mCT PET/CT scanner (Siemens Medical Solutions, Knoxville, TN, USA) with an acquisition time of 3 min per bed position, covering an extended field of view (FOV) of 21.4 cm. The images were iteratively reconstructed using a 3-dimensional OSEM (ordered-subset expectation maximization) algorithm (3 iterations; 24 subsets) with 5 mm gaussian filtering and slice thickness of 5 mm. A standard low-dose spiral CT was acquired for

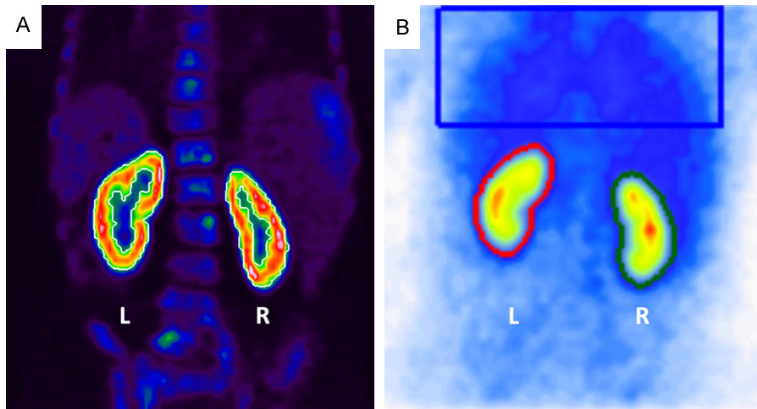


Figure 1. A. Renal PSMA quantification. SUV-threshold for selection of renal tissue was set at 30% of SUVmax using auto-contouring (white). Renal pelvic activity such as in obstructive nephropathy was manually excluded from analysis. B. Renal MAG3 with ROI placement (left kidney: red, right kidney: green, background: blue).

Table 2. Descriptive statistics of split renal function of the right kidney measured by PSMA PET imaging and by standard renal scintigraphy

| Type of Measurement | Mean (%) | SD (%) | Min (%) | Max (%) |
|--------------------------------------|----------|--------|---------|---------|
| ⁶⁸ Ga-PSMA-11 PET | 50.5 | 13.2 | 4.5 | 99.7 |
| ^{99m} Tc-MAG-3 scintigraphy | 50.3 | 13.0 | 11.4 | 96.8 |

attenuation correction and anatomical localization using an x-ray tube voltage of 120 keV and a modulation of the tube current using CARE Dose4D with a maximal tube current time product of 30 mAs. To calculate relative PSMA distribution in both kidneys volumes of interest were used (VOI), drawn and generated using the *syngo.via* software (Siemens Healthineers, Erlangen, Germany). Each VOI was manually drawn as to contain the kidney. Setting a threshold of 30% of the maximum standard uptake volume (SUVmax) was best suited to delineate the renal tissue in the selected area by autocontouring, as shown in **Figure 1A**. Accuracy of the auto-contouring tool was controlled visually by comparing the results with the actual kidney size on low-dose CT. If non-renal tissue was within the selection (i.e. tracer retention in the renal pelvis) it was cropped and removed manually. The volume and the mean standard uptake value (SUVmean) were then used for calculating of SRF: $SRF_{right} = (volume_{right} \times SUVmean_{right}) / (volume_{right} \times SUVmean_{right} + volume_{left} \times SUVmean_{left})$.

^{99m}Tc-MAG3 scintigraphy: Each patient of this study (n=97) received renal scintigraphy with a

mean intravenously injected activity of 99.4 ± 13.4 MBq of ^{99m}Tc-MAG3. Dynamic images starting at time of injection were acquired using a Diacam Scintron (MiE medical imaging electronics, Seth, Germany) with a low energy high-resolution collimator (LEHR). MiE software was used for data analysis. Manual regions of interest (ROI) were drawn closely around each kidney. Background correction (rectangular ROI placed in the thorax region) was applied. SRF_{MAG3} was calculated based on the renal secretion phase (first 2 minutes) using integral method, which is described in detail in [21]. Standard furosemide administration after 30 min in cases of renal retention with subsequent 20 min imaging was performed to check for reno-ureteral obstruction.

Statistical analysis

For statistical analysis, Pearson's correlation coefficient was used to measure the strength of the relationship of both methods of SRF calculation. A two-sided *p*-value < 0.05 was considered statistically significant. In addition, a Bland-Altman-Plot [22, 23] was generated to assess the agreement between both methods. Limits of agreement were set with a confidence interval (CI) of 95%. Statistical analysis was conducted using IBM SPSS Statistics 25.

Results

Mean SRF of the right kidney was 50.5 % (range: 4.5-99.7%) and 50.3% (range: 11.4-96.8%) using PSMA PET/CT and MAG3 scintigraphy, respectively. **Table 2** presents descriptive statistics of our data. The correlation between PSMA and MAG3 derived SRF was highly significant (*P* < 0.001) with a correlation coefficient of *r*=0.91 (**Figure 2A**). The Bland-Altman plot analysis (**Figure 2B**) shows an agreement of the highly correlated measurements with a mean difference of 0.002 [CI -0.110; 0.114]. This agreement was also observed visually; **Figure 3** shows two representative cases.

PSMA PET based split renal function

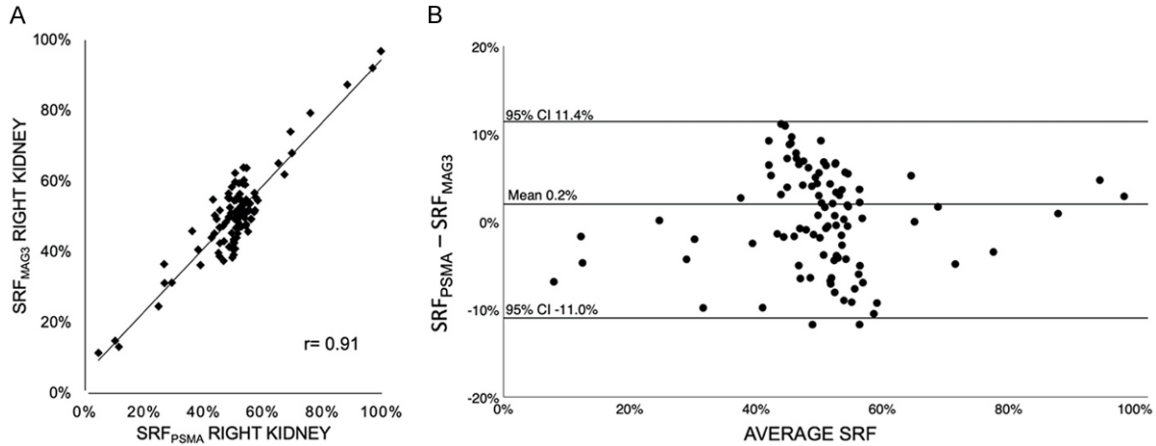


Figure 2. (A) Pearson correlation coefficient ($r=0.91$, $P < 0.001$) and (B) Bland-Altman-Plot of SRF_{PSMA} and SRF_{MAG3} of the entire cohort ($n=98$).

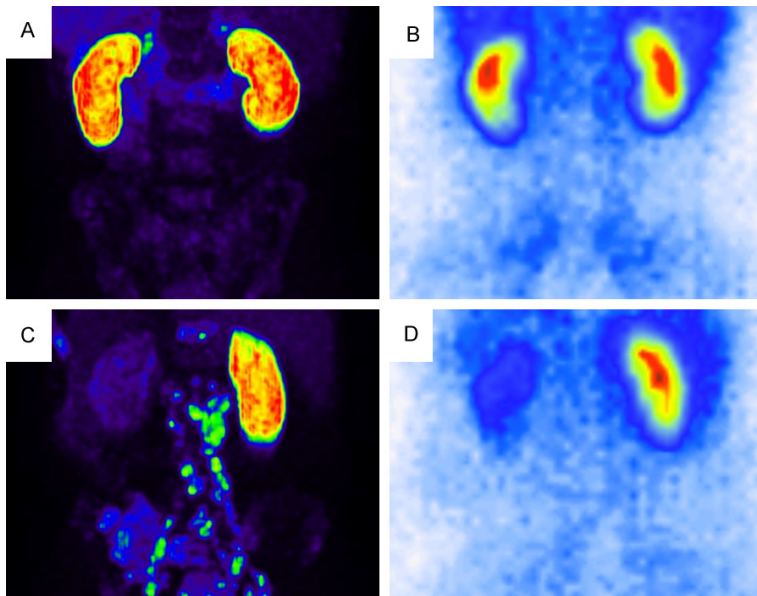


Figure 3. Example of two representative cases with bilaterally equal SRF (A) PSMA PET [$SRF_{right} : 49.9\%$], (B) MAG3 scintigraphy [$SRF_{right} : 48.4\%$] and laterally different SRF (C) PSMA PET [$SRF_{right} : 79.3\%$], (D) MAG3 scintigraphy [$SRF_{right} : 76.0\%$].

As illustrated in **Figures 4** and **5**, in both subgroup analyses of $n=77$ patients with normal renal function ($eGFR \geq 60$ ml/min), and $n=20$ patients with reduced renal function ($eGFR < 60$ ml/min) a high correlation of both methods was seen ($r=0.83$, $P < 0.001$ and $r=0.98$, $P < 0.001$), as well as an agreement in the Bland-Altman analysis (mean: -0.002 [CI -0.118 ; 0.116], mean: 0.018 [CI -0.072 ; 0.108]). Unilateral reno-ureteral obstruction defined by standard criteria as $> 50\%$ renal tracer reten-

tion in MAG3 scintigraphy 20 min after furosemide administration was observed in 14 patients. In 13 of these 14 patients (92.9 %) obstruction was visually discernable on PSMA imaging. **Figure 6** illustrates a representative case for this aspect.

Discussion

As a proof of principle, this retrospective study on $n=97$ patients with dual assessment by ^{68}Ga -PSMA-11 PET and standard renal scintigraphy with ^{99m}Tc -MAG3 demonstrates that PSMA-targeted radioligand imaging allows assessment of split renal function (SRF). We provide a preliminary first proof that renal PSMA expression in the proximal tubules of the kidney

is a surrogate marker of functional renal tissue.

The calculated highly significant correlation ($r=0.91$, $P < 0.001$) of SRF_{PSMA} and SRF_{MAG3} is similar to other established renal function assessment methods. ^{99m}Tc -DMSA and ^{99m}Tc -MAG3 scintigraphy achieved correlations in the range of $r=0.82$ - 0.99 [24-27]. Other reported approved methods of SRF assessment are within the same range of correlation [28-31].

PSMA PET based split renal function

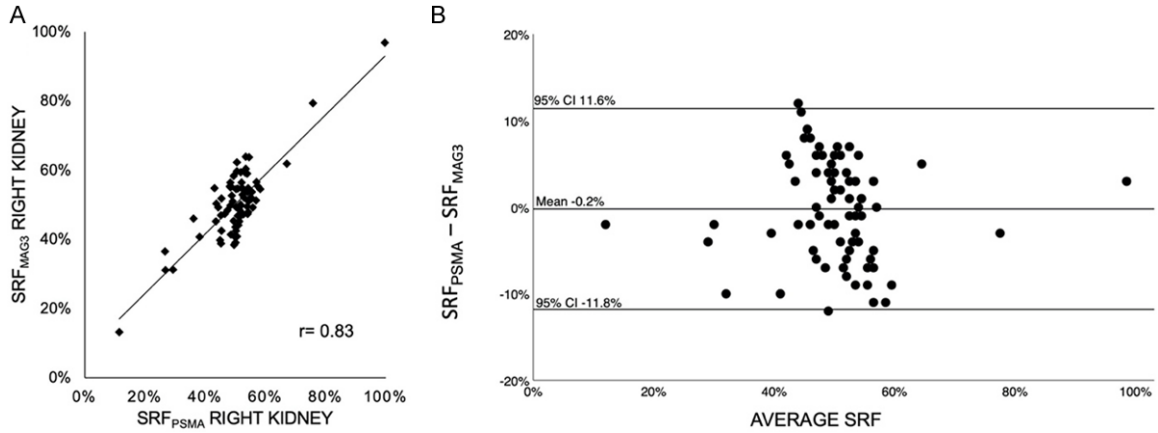


Figure 4. (A) Pearson correlation coefficient ($r=0.83$, $P < 0.001$) and (B) Bland-Altman-Plot of SRF_{PSMA} and SRF_{MAG3} in patients ($n=77$) with normal renal function ($GFR \geq 60$ ml/min).

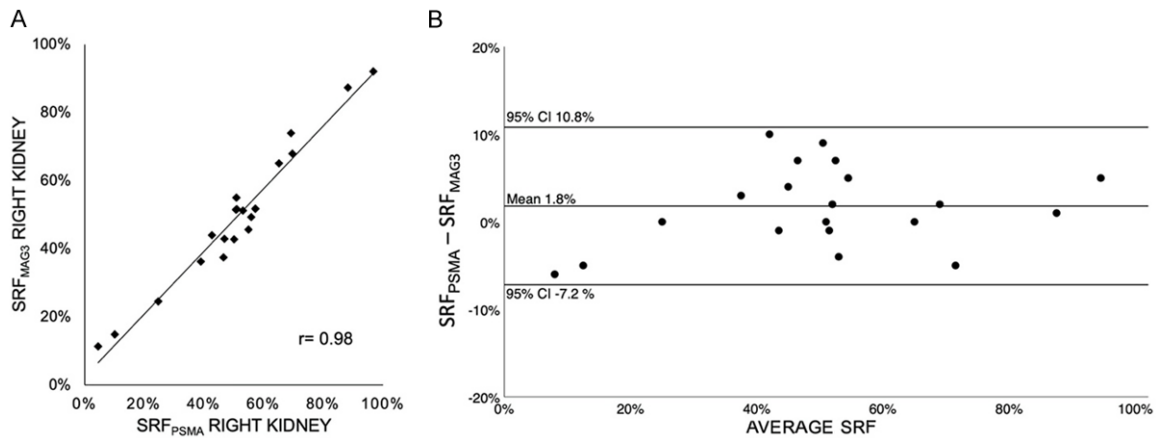


Figure 5. (A) Pearson correlation coefficient ($r=0.98$, $P < 0.001$) and (B) Bland-Altman-Plot of SRF_{PSMA} and SRF_{MAG3} in patients ($n=20$) with reduced renal function ($GFR < 60$ ml/min).

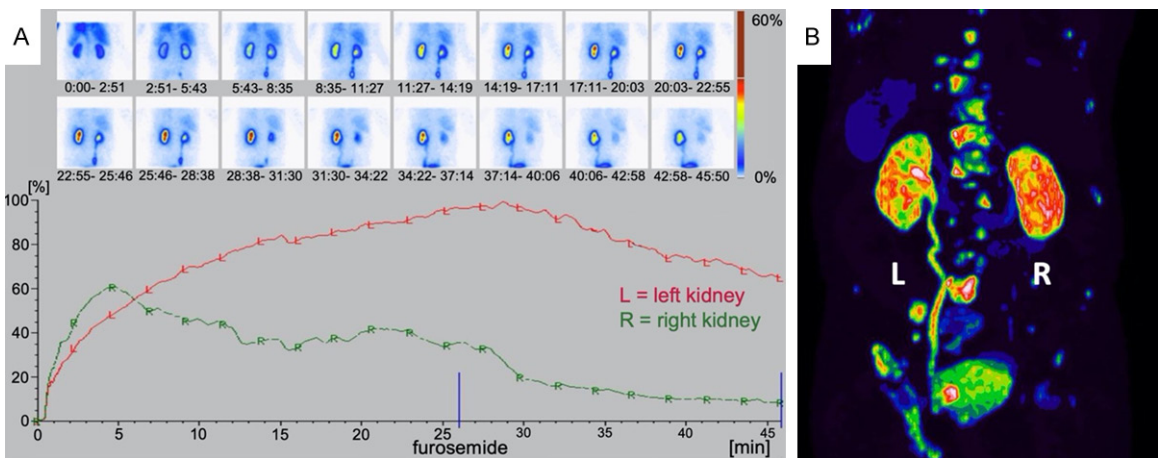


Figure 6. Example of reno-ureteral obstruction seen in a patient; A. MAG3 scintigraphy revealing tracer retention of $> 50\%$ on the left side after furosemide administration, B. PSMA PET showing intense tracer accumulation in the dilated left ureter and renal pelvis.

Table 3. Reported correlations between different methods of split renal function assessment

| Study | Year | N | Method 1 | Method 2 | Correlation |
|---------------------|------|-------|----------------|----------|-------------|
| Piepsz et al. | 1978 | n=19 | Renal catheter | DTPA | 0.94 |
| Chanard et al. | 1982 | n=14 | Renal catheter | DTPA | 0.94 |
| Llams-Elvira et al. | 1989 | n=100 | MAG3 | DMSA | 0.97 |
| Bair et al. | 1995 | n=37 | MAG3 | DMSA | 0.82-0.99 |
| Ardela Díaz et al. | 2002 | n=138 | MAG3 | DMSA | 0.92-0.96 |
| Miyazaki et al. | 2010 | n=60 | DMSA | DTPA | 0.83 |
| Aktaş et al. | 2010 | n=19 | MAG3 | DMSA | 0.84 |
| Momin et al. | 2018 | n=50 | DMSA | DTPA | 0.99 |
| Present study | 2020 | n=97 | PSMA | MAG3 | 0.91 |

Table 3 compiles SRF correlations between two different methods reported in literature. With a Bland-Altman analysis revealing a mean difference of 0.002 with 95%-CI of [-0.110; 0.114] our results suggest that PSMA-derived SRF is in good agreement with the established MAG3 scintigraphy-derived SRF. A variance up to in the order of 10% within the largely symmetrical bilateral renal function range (40-60% SRF) is clinically less relevant and seen within other historical comparison of established methods of SRF assessment [30, 31]. Asymmetrical renal function distribution is very accurately quantified by PSMA imaging. In addition, the correlation and Bland-Altman agreement of SRF_{PSMA} and SRF_{MAG3} is not affected by renal function, as indicated by our subgroup analysis of patients with normal and reduced renal function showing similar results.

Another observation in our study was the depiction of reno-ureteral obstruction by PSMA imaging in most cases (92.9%), which encourages the thorough PET reading in this regard.

The presented results of this study are of particular interest in pre- and post-treatment management of mCRPC patients, in which PSMA PET/CT is a frequently performed imaging method for staging and restaging. With the presented new insights, these PSMA-PET/CTs can be used to calculate SRF at baseline of PSMA-RLT and to detect unilateral changes during follow-up, potentially induced by tumor-obstructive nephropathies or therapy-induced nephrotoxicity. Additional MAG3 scintigraphy might be dispensable, as shown by our study, sparing patients from unnecessary radiation exposure and distress.

Limitations

The retrospective nature and the number of patients (n=97) may limit the strength of conclusions. The study comprises no representative cross-section of normal population, as only men with advanced, metastasized castration-resistant prostate cancer were investigated. This may be seen as another limitation for generalizing conclusions.

A larger confirmatory study would be highly warranted to confirm the results.

Conclusion

Renal tubular PSMA expression allows assessment of split renal function (SRF) by ⁶⁸Ga-PSMA-11 PET/CT imaging. SRF derived by PSMA PET and MAG3 scintigraphy are in good agreement. Additional MAG3 scintigraphy in order to quantify relative renal function contribution may be spared; larger analyses are warranted to confirm our findings and establish this approach to save time, distress and unnecessary radiation exposure for the patients.

Disclosure of conflict of interest

None.

Address correspondence to: Dr. Samer Ezziddin, Department of Nuclear Medicine, Saarland University Hospital, Kirrberger Street Geb. 50, D-66421 Homburg, Germany. Tel: +49 6841 16 22201; Fax: +49 6841 16 17 24595; E-mail: samer.ezziddin@uks.eu

References

- [1] Torre LA, Bray F, Siegel RL, Ferlay J, Lortet-Tieulent J and Jemal A. Global cancer statistics, 2012. *CA Cancer J Clin* 2015; 65: 87-108.
- [2] Beckett ML, Cazares LH, Vlahou A, Schellhammer PF and Wright GL. Prostate-specific membrane antigen levels in sera from healthy men and patients with benign prostate hyperplasia or prostate cancer. *Clin Cancer Res* 1999; 5: 4034-40.
- [3] Ghosh A and Heston WD. Tumor target prostate specific membrane antigen (PSMA) and

PSMA PET based split renal function

- its regulation in prostate cancer. *J Cell Biochem* 2004; 91: 528-39.
- [4] Israeli RS, Powell CT, Corr JG, Fair WR and Heston WD. Expression of the prostate-specific membrane antigen. *Cancer Res* 1994; 54: 1807-11.
- [5] Heston WD. Characterization and glutamyl preferring carboxypeptidase function of prostate specific membrane antigen: a novel folate hydrolyase. *Urology* 1997; 49: 104-12.
- [6] Afshar-Oromieh A, Babich JW, Kratochwil C, Giesel FL, Eisenhut M, Kopka K and Haberkorn U. The rise of PSMA ligands for diagnosis and therapy of prostate cancer. *J Nucl Med* 2016; 57: 79S-89S.
- [7] Eissa A, Elsherbiny A, Coelho RF, Rassweiler J, Davis JW, Porpiglia F, Patel VR, Prandini N, Micali S, Sighinolfi MC, Puliatti S, Rocco B and Bianchi G. The role of ⁶⁸Ga-PSMA PET/CT scan in biochemical recurrence after primary treatment for prostate cancer: a systematic review of the literature. *Minerva Urol Nefrol* 2018; 70: 462-78.
- [8] Verburg FA and Pfestroff A. PSMA PET-CT in initial prostate cancer staging. *Nat Rev Urol* 2016; 13: 498-9.
- [9] Ceci F, Herrmann K, Hadaschik B, Castellucci P and Fanti S. Therapy assessment in prostate cancer using choline and PSMA PET/CT. *Eur J Nucl Med Mol Imaging* 2017; 44: 78-83.
- [10] Heinzel A, Boghos D, Mottaghy FM, Gaertner F, Essler M, von Mallek D and Ahmadzadehfar H. ⁶⁸Ga-PSMA PET/CT for monitoring response to ¹⁷⁷Lu-PSMA-617 radioligand therapy in patients with metastatic castration-resistant prostate cancer. *Eur J Nucl Med Mol Imaging* 2019; 46: 1054-62.
- [11] Kim YJ and Kim Y. Therapeutic responses and survival effects of ¹⁷⁷Lu-PSMA-617 radioligand therapy in metastatic castrate-resistant prostate cancer: a meta-analysis. *Clin Nucl Med* 2018; 43: 728-34.
- [12] Fendler WP, Rahbar K, Herrmann K, Kratochwil C and Eiber M. ¹⁷⁷Lu-PSMA radioligand therapy for prostate cancer. *J Nucl Med* 2017; 58: 1196-200.
- [13] Rajasekaran AK, Anilkumar G and Christiansen JJ. Is prostate-specific membrane antigen a multifunctional protein? *Am J Physiol Cell Physiol* 2005; 288: C975-81.
- [14] Kinoshita Y, Kuratsukuri K, Landas S, Imaida K, Rovito PM Jr, Wang CY and Haas GP. Expression of prostate-specific membrane antigen in normal and malignant human tissues. *World J Surg* 2006; 30: 628-36.
- [15] Silver DA, Pellicer I, Fair WR, Heston WD and Cordon-Cardo C. Prostate-specific membrane antigen expression in normal and malignant human tissues. *Clin Cancer Res* 1997; 3: 81-5.
- [16] Forrer F, Rolleman E, Bijster M, Melis M, Bernard B, Krenning EP and de Jong M. From outside to inside? Dose-dependent renal tubular damage after high-dose peptide receptor radionuclide therapy in rats measured with in vivo ^{99m}Tc-DMSA-SPECT and molecular imaging. *Cancer Biother Radiopharm* 2007; 22: 40-9.
- [17] Violet J, Jackson P, Ferdinandus J, Sandhu S, Akhurst T, Irvani A and Kong G, Kumar AR, Thang SP, Eu P, Scalzo M, Murphy D, Williams S, Hicks RJ and Hofman MS. Dosimetry of ¹⁷⁷Lu-PSMA-617 in Metastatic castration-resistant prostate cancer: correlations between pretherapeutic imaging and whole-body tumor dosimetry with treatment outcomes. *J Nucl Med* 2019; 60: 517-23.
- [18] Yordanova A, Becker A, Eppard E, Kürpig S, Fissang C, Feldmann G, Essler M and Ahmadzadehfar H. The impact of repeated cycles of radioligand therapy using [¹⁷⁷Lu]Lu-PSMA-617 on renal function in patients with hormone refractory metastatic prostate cancer. *Eur J Nucl Med Mol Imaging* 2017; 44: 1473-9.
- [19] Levey AS. A more accurate method to estimate glomerular filtration rate from serum creatinine: a new prediction equation. *Ann Intern Med* 1999; 130: 461-70.
- [20] Fritzberg AR, Kasina S, Eshima D and Johnson DL. Synthesis and biological evaluation of technetium-99m MAG3 as a hippuran replacement. *J Nucl Med* 1986; 27: 111-6.
- [21] Piepsz A, Tondeur M and Ham H. Relative ^{99m}Tc-MAG3 renal uptake: reproducibility and accuracy. *J Nucl Med* 1999; 40: 972-6.
- [22] Bland JM and Altman DG. Statistical methods for assessing agreement between two methods of clinical measurement. *Lancet* 1986; 1: 307-10.
- [23] Giavarina D. Understanding bland altman analysis. *Biochem Med* 2015; 25: 141-51.
- [24] Llamas-Elvira JM, Martinez-Paredes M, Jimenez-Heffernan A, Sopena R, Requena MJ, Gonzalez FM, Torres M and Mateo A. ^{99m}Tc-MAG3 for quantitation of differential renal function. *Nucl Med Commun* 1989; 10: 759-64.
- [25] Bair HJ, Becker W, Schott G, Kühn RH and Wolf F. Is there still a need for Tc-99m DMSA renal imaging? *Clin Nucl Med* 1995; 20: 18-21.
- [26] Ardela Díaz E, Miguel Martínez B, Gutiérrez Dueñas JM, Díez Pascual R, García Arcal D and Domínguez Vallejo FJ. Comparative study of differential renal function by DMSA and MAG-3 in congenital unilateral uropathies. *Cir Pediatr* 2002; 15: 118-21.
- [27] Aktaş GE and Inanir S. Relative renal function with MAG-3 and DMSA in children with unilat-

PSMA PET based split renal function

- eral hydronephrosis. *Ann Nucl Med* 2010; 24: 691-5.
- [28] Piepsz A, Denis R, Ham HR, Dobbeleir A, Schulman C and Erbsmann F. A simple method for measuring separate glomerular filtration rate using a single injection of ^{99m}Tc -DTPA and the scintillation camera. *J Pediatr* 1978; 93: 769-74.
- [29] Chanard J, Ruiz JC, Liehn JC, Lemaire P, Brunois JP, Lardennois B and Valeyre J. Assessment of divided renal function by renography. Validation in patients with separate urine collections from each kidney. *Clin Nephrol* 1982; 18: 291-6.
- [30] Miyazaki C, Harada H, Shuke N, Okizaki A, Miura M and Hirano T. ^{99m}Tc -DTPA dynamic SPECT and CT volumetry for measuring split renal function in live kidney donors. *Ann Nucl Med* 2010; 24: 189-95.
- [31] Momin MA, Abdullah MNA and Reza MS. Comparison of relative renal functions calculated with ^{99m}Tc -DTPA and ^{99m}Tc -DMSA for kidney patients of wide age ranges. *Phys Med* 2018; 45: 99-105.